Impact of evolving fabric anisotropy on CPT simulations for subsurface characterization

Sara Moshfeghi[1], *Mahdi* Taiebat[1#] *and Arcesio* Lizcano[2]

[1]*Department of Civil Engineering, University of British Columbia, Vancouver, BC, Canada*
[2]*SRK Consulting Inc., Vancouver, BC, Canada*
[#]*Corresponding author: mtaiebat@civil.ubc.ca*

ABSTRACT

In geotechnical site characterization, Cone Penetration Testing (CPT) is a fundamental method for evaluating subsurface conditions of granular materials such as sands, silts, and non-plastic tailings. This study advances CPT simulations by incorporating the fabric anisotropy variable A into the SANISAND-F model and utilizing the Material Point Method (MPM), with a specific focus on the role of evolving fabric within an anisotropic critical state framework. The objective is to deepen the understanding of how the evolving fabric of soils influences macroscopic site characterization outcomes. Through carefully controlled initial conditions, including void ratio and confining pressure, the study aims to demonstrate the impact of fabric anisotropy on CPT resistance measurements. Assessment of the evolution of material state based on the key constitutive ingredient of the model allows for explaining the reason behind the respective values of cone tip resistance observed from the CPT simulations, considering fabric anisotropy and the anisotropic critical state framework. This approach enhances the modeling of this site characterization method, providing a more comprehensive framework for interpreting soil mechanical behavior and enhancing predictive modeling capabilities.

Keywords: CPT; material point method; critical state; fabric anisotropy; sand.

1. Introduction

The Cone Penetration Test (CPT) is a dominant field-based method in geotechnical engineering for subsurface characterization. It involves pushing a cone into the soil layer and measuring resistance, providing valuable data for identifying soil types and properties. Over the years, researchers have developed approximate empirical formulas and charts to interpret CPT data for classifying sands and clays. These formulas and charts are derived from two main sources: firstly, a blend of lab element tests on certain soil samples and controlled tests in larger soil chambers, and secondly, retrospective analyses of previous case studies based on limit equilibrium analysis and correlating the back-calculated strength properties to CPT tests data.

There is, however, a growing need within the geotechnical community to extract more detailed information from CPT data, especially for different types of soils such as sands, silts, and non-plastic tailings from mining processes. This demand has led to an increased interest in the mechanics-based interpretation of CPT using validated numerical modeling as a means to simulate the CPT process more accurately. Recent advancements in detailed numerical simulations of CPT have contributed to a better understanding

of the CPT measurement and the related in-situ soil conditions (e.g., Ghasemi et al., 2018; Martinelli and Galavi, 2021; Monforte et al., 2022; Pezeshki and Ahmadi, 2022; Yost et al., 2022). Successful numerical modeling of CPT requires at least two main elements: robust computational techniques capable of handling large deformation problems, and representative constitutive models that capture various important aspects of soil response.

Among the computational techniques adopted for CPT simulations are the Arbitrary Lagrangian-Eulerian (ALE) techniques, the Particle Finite Element Method (PFEM), and the Material Point Method (MPM). Each technique offers its advantages in terms of flexibility and precision, but also comes with specific challenges, including ensuring accuracy. Despite their challenges, these methods have proven to be effective in advancing our ability to simulate the CPT, particularly in dealing with the associated large deformations.

Numerical modeling efforts for simulating the CPT have largely relied on basic constitutive models such as Mohr-Coulomb and its variants, which fall short of capturing the complex stress-strain behavior of soils. Recognizing this limitation highlights the critical need for more advanced simulations that can more accurately reflect the soil's stress-strain response, and in line with that need, there is a growing body of works utilizing more representative soil models (e.g., Fan et al., 2018; Kouretzis et al., 2014; Martinelli and Pisano, 2022; Monforte et al., 2022; Salgado et al., 2022). The pursuit of enhancing CPT simulations by integrating more complex models remains a key research priority, aiming to achieve a more precise representation of soil mechanics.

Recent contributions by Moshfeghi et al. (2023) utilize the MPM technique to examine the impact of soil constitutive models on CPT simulations, specifically comparing the DM04 (Dafalias and Manzari, 2004) against the elastic perfectly plastic Drucker-Prager model

in varied sand densities. The study underscores DM04's advanced capabilities, including nonlinear elasticity, hardening/softening, contractancy/dilatancy, and a critical state framework, in effectively capturing soil's complex responses, thereby influencing CPT results. Their results highlight that beyond material strength, factors like soil stiffness and stress path experienced during the penetration process significantly affect the recorded cone tip resistance as well. In follow-up work, Moshfeghi et al. (2024) further validated the use of the MPM and DM04 model by correlating the sand state parameter with cone tip resistance, comparing simulation outcomes to physical model data in a calibration chamber. This comparison showed the simulations were reasonably successful in reflecting actual behavior observed during cone penetration tests, particularly in dense states of a reference clean sand. However, despite the lack of data across all densities, the accuracy of simulations appeared to decline in looser sand states, as indicated by trends.

This paper presents preliminary results from utilizing a more advanced version of the DM04 model, specifically the SANISAND-F model proposed by Petalas et al. (2020), with a primary focus on the role of the fabric anisotropy variable A. This variable acts as a scalar measure of the alignment between an evolving fabric tensor and the direction of deviatoric plastic strain rate. The enhancement of SANISAND-F over DM04 is initially demonstrated through comparative simulations of element-level tests on medium-dense to loose Toyoura sand samples in undrained and drained triaxial tests, and subsequently through simulations of CPT in dry Toyoura sand. Specifically, it assesses the impact of SANISAND-F's advanced constitutive features on simulating cone tip resistance, preparing the ground for a detailed discussion on its role in enhancing the accuracy of CPT simulations accounting for soil fabric anisotropy.

2. Constitutive models

The DM04 model by Dafalias and Manzari (2004), characterized by its critical state compatibility and stress-ratio controlled bounding surface plasticity, laid the groundwork for what was later named the SANISAND class of models by Taiebat and Dafalias (2008). The SANISAND-F model, a recent addition to this class introduced by Petalas et al. (2020), expands upon these principles within the Anisotropic Critical State Theory (ACST) framework, as described by Li and Dafalias (2012). By incorporating fabric effects, the SANISAND-F model enhances the predictive capabilities for the anisotropic behavior of sands, marking a significant evolution in the SANISAND series at the cost of three additional model parameters.

In ACST, the variable A signifies fabric anisotropy, defined by the trace of the fabric tensor and plastic strain rate direction product, achieving a critical value of 1 in the critical state. This variable A contributes to the formulation of the dilatancy state parameter (DSP) ζ, replacing the traditional isotropic state parameter ψ in defining both dilatancy and the plastic modulus. Predominantly through ζ, and supplemented by the plastic modulus and fabric evolution rate's dependence on A, the SANISAND-F model effectively models the anisotropic responses of sand under drained and undrained shearing conditions.

The fabric anisotropy is represented through the deviatoric fabric tensor state variable $\boldsymbol{F} = F\boldsymbol{n}_F$, where F stands for the tensor's norm and $\boldsymbol{n}_F$ its unit direction. This tensor can potentially be linked to the statistical orientation of particles, contact normals, or void spaces within a granular matrix. Its initial value is characterized by its norm F_{in} and directional vector $\boldsymbol{n}_F$. The tensor $\boldsymbol{R}'$, aligned with the deviatoric plastic strain rate tensor, establishes ACST's loading direction through the unit-norm deviatoric tensor $\boldsymbol{n}' = \boldsymbol{R}'/|\boldsymbol{R}'|$, where $|\boldsymbol{R}'|$ quantifies its magnitude. The scalar $A = \boldsymbol{F}:\boldsymbol{n}'$ serves to quantify fabric anisotropy variable.

For sand samples prepared by any method (e.g., pluviation, tamping, etc.) and oriented with respect to the vertical z axis and the horizontal x–y plane of deposition, the initial transverse isotropy of the fabric tensor $\boldsymbol{F}$ is defined by its norm, F_{in}, and the principal values of its unit-norm direction $\boldsymbol{n}_F$. Specifically, these are $n_{Fzz} = n_{F1} = 2/\sqrt{6}$ for the vertical direction, and $n_{Fxx} = n_{Fyy} = n_{F2} = n_{F3} = -1/\sqrt{6}$ for the horizontal directions. Referencing some of the recent efforts for quantifying its values, Petalas et al. (2020) employed an F_{in} value of 0.5, within a range of $F_{in} = 0\text{–}0.6$, for simulations of Toyoura sand in element level tests across various preparation methods. This choice of a consistent F_{in} value was a strategic simplification to explore the model's simulation effectiveness without detailed tuning of the F_{in} value, which could yield marginally improved simulations. This simplified approach is also followed in the current paper.

Table 1 presents the constants of the DM04 and SANISAND-F models for Toyoura sand, adopted from Dafalias and Manzari (2004) and Petalas et al. (2020), respectively. The fabric-dilatancy feature in the DM04 model has been deactivated to provide a clearer view of the effects of fabric anisotropy. To reduce the impact of stress oscillations from MPM analysis on induced plasticity, the model parameter governing the size of the conical yield surface is set to $m = 0.1$.

Table 1. Material constants of DM04 and SANISAND-F models and their values for Toyoura sand.

Model	DM04		SANISAND-F*	
constant	Symbol	Value	Symbol	Value
Elasticity	G_0	125	G_0	125
	ν	0.05	ν	0.05
Critical state	M_c	1.25	M	1.25
	c	0.712	c	0.75
	e_c^{ref}	0.934	e_c^{ref}	0.934
	λ_c	0.019	λ_c	0.019
	ξ	0.7	ξ	0.7
Yield surf.	m	0.1	m	0.1
Plastic modulus	h_0	7.05	h_1	7.5
	c_h	0.968	c_h	0.85
	n^{b}	1.1	n^{b}	1.4
Dilatancy	A_0	0.704	A_0	0.704
	n^{d}	3.5	n^{d}	3.5
Fabric anisotropy	–	–	e_A	0.0818
	–	–	c_0	5.2
	–	–	h_2	1.3

* Initial values of state variables:
F_{in}=0.5; $\boldsymbol{n}_F$=$[2/\sqrt{6}, -1/\sqrt{6}, -1/\sqrt{6}, 0, 0, 0]$

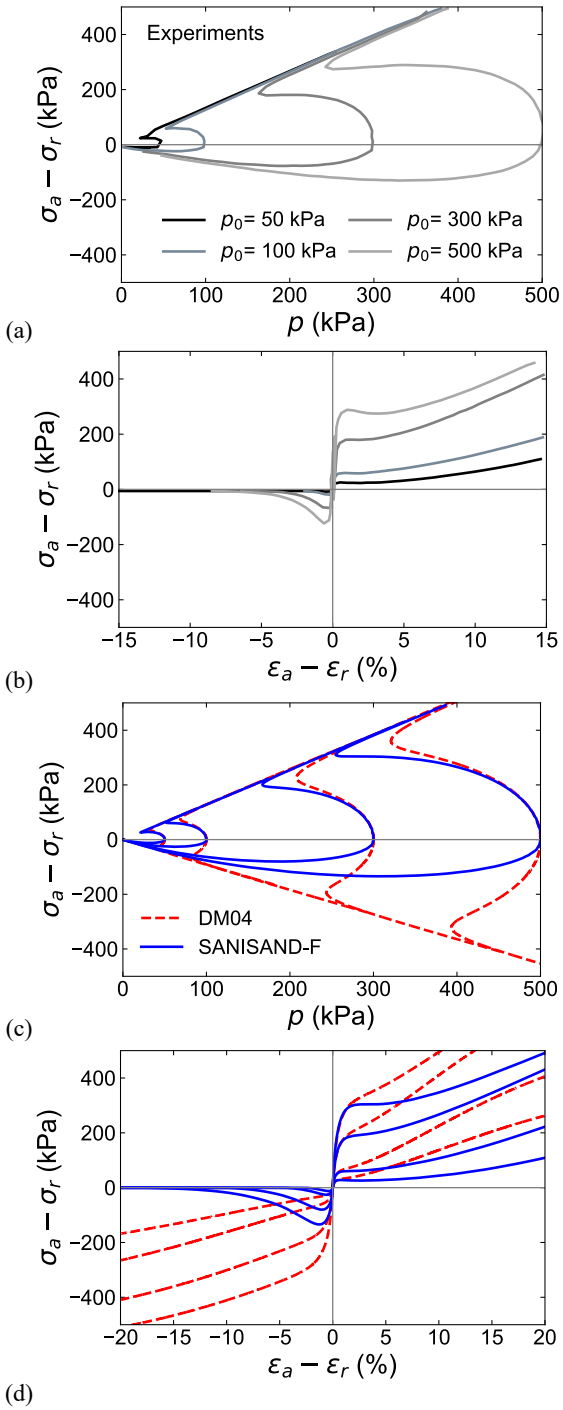

Figure 1. Comparison of (a,b) experimental data on Toyoura sand in undrained triaxial compression and extension at e_0=0.86–0.89 and different levels of p_0 in the range of 50 to 500 kPa (Yoshimine et al., 1998), against (c,d) DM04 and SANISAND-F model simulations.

Figure 1 illustrates a detailed comparison between simulations of the DM04 and SANISAND-F models, alongside experimental data from Yoshimine et al. (1998), as also presented in Bokkisa et al. (2022). The comparison focuses on undrained triaxial compression and extension loading tests conducted on Toyoura sand with varying void ratios and stress levels. The experimental data presented included samples with initial void ratios (e_0) in the range 0.86–0.89. The initial mean effective stress (p_0) varied from 50 to 500 kPa. Note that all stresses presented in this paper are effective. This figure shows that both models adequately capture the

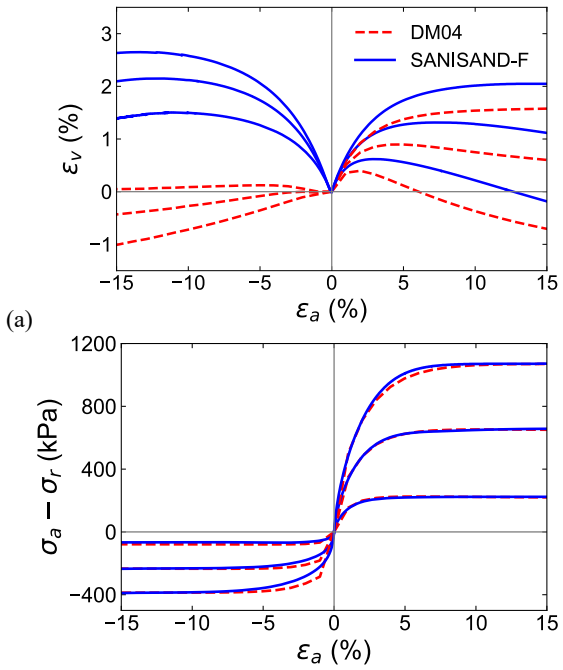

Figure 2. Comparison of DM04 and SANISAND-F model simulations in drained triaxial compression and extension at e_0 = 0.88 and different levels of p_0 in the range of 100 to 500 kPa.

compression tests. However, SANISAND-F simulations outperform DM04 simulations by accurately representing the contractive response in the extension tests, whereas DM04 simulations inaccurately exhibit a dilative response in the extension tests.

Figure 2 depicts simulations of drained triaxial compression and extension loading tests using the model parameters for Toyoura sand. The simulations started from a void ratio of 0.88, and the initial mean effective stress was varied from 100 to 500 kPa. Similar to the observations in the undrained tests presented in Fig. 1, the two models exhibit fairly comparable simulation results for triaxial compression, but their responses noticeably differ in the extension tests. While this figure does not present a comparison with experimental data, relying on the more representative response of SANISAND-F in Fig. 1, one may conclude that the more contractive (and less dilative) response presented by the SANISAND-F model in Fig. 2 to be in line with the actual response of Toyoura sand in drained shearing.

3. CPT model description

A 2D-axisymmetric numerical model was developed using the ANURA3D platform (Anura3D, 2022) to investigate the soil response to cone penetration. Figure 3 presents the numerical model configuration, including the MPM compressing and moving mesh, the schematic geometry and boundary conditions of the cone-soil domain, and the positioning of a control material point (CMP). The selected CMP is at an initial depth of $z = 20r_c$ and radial distance of $r = 0.5r_c$. It also highlights the depth of the cone tip, z_t, at the start and conclusion of the simulation. The soil domain was subjected to a 140 kPa surcharge, with the initial coefficient of lateral to vertical stress ($K_{h,in}$) set at 0.5. Gravity was excluded

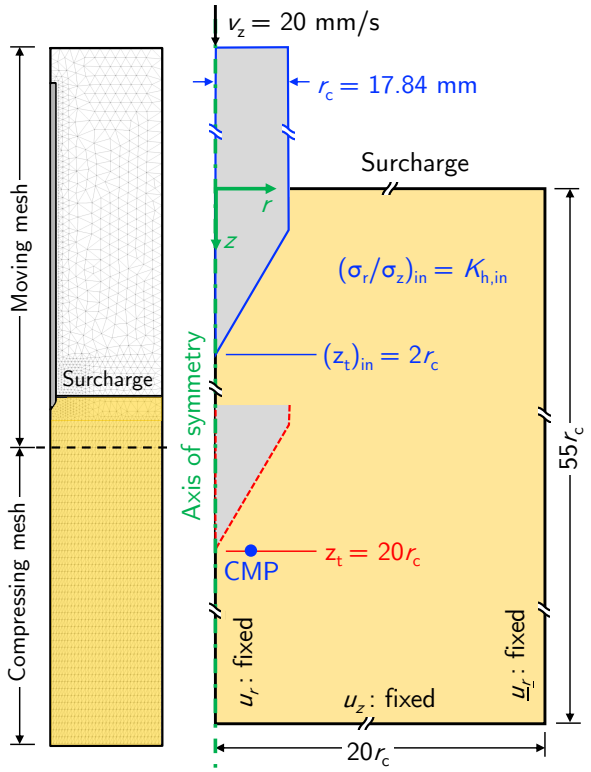

Figure 3. Numerical model configuration: MPM mesh, schematic geometry and boundary conditions of cone-soil domain, control material point (CMP) location, and cone tip depth z_t at simulation start and end.

from the analysis to maintain constant initial stress across the model's depth. The soil domain was simulated using both DM04 and SANISAND-F, calibrated for Toyoura sand with the same model constants presented in Table 1, and a void ratio of 0.88.

The cone, conforming to standard specifications with a radius of $r_c = 17.84$ mm and an apex angle of 60 degrees, was embedded to a depth of $2r_c$. To circumvent numerical instabilities, the cone's tip and its junction with the shaft were slightly rounded. The cone was modeled as a rigid body descending at a specified velocity v_z. Its interaction with the soil is described by the algorithm proposed by Bardenhagen (2001), featuring an interface friction angle of 21 degrees. To reduce stress oscillations, a homogeneous local damping of 10% was adopted. Additionally, the strain smoothing technique suggested by Al-Kafaji (2013) was applied to prevent the locking of elements.

The numerical integration for the DM04 and SANISAND-F models utilized a modified Euler method with auto sub-stepping and error control. A 1×10^{-4} s time increment was adopted for all simulations based on the penetration velocity of 20 mm/s, the critical time-step of approximately 1×10^{-3} s due to chosen discretization and material model stiffness, and to ensure precise numerical integration.

Spatial discretization leveraged a moving mesh technique to maintain a finely meshed area around the cone tip throughout the simulation, ensuring detailed geometry within the contact zone between the cone and soil for efficient computations. The mesh density is finer near the cone tip and becomes coarser away from it to reduce computational demands, with the boundary between moving and compressing mesh located at $z = 8r_c$. To ensure simulation accuracy and avoid empty elements, which could lead to errors, the number of material points per element (MP/El) is carefully managed. Around the cone tip, a density of 25 MP/El was employed, which is reduced to 12 and 6 MP/El as the distance from the cone's centerline increases. This gradation supports computational efficiency while maintaining model integrity. A specific control material point at an initial depth of $z = 20r_c$ and radial distance of $r = 0.5r_c$, designated as CMP, facilitates detailed analysis of the material state evolution during cone penetration.

4. Results and discussion

Figure 4 presents the cone tip resistance values obtained from simulations using the DM04 and SANISAND-F models. The cone tip resistance values were determined based on the vertical reaction recorded at the cone area during penetration. The values are reported with respect to the normalized penetration depth z_t/r_c, where z_t represents the depth of the cone tip, and r_c represents the cone radius, following the illustration presented earlier in Fig 3. The simulations were continued until the normalized penetration depth z_t/r_c reached 20, indicating that the cone tip had reached the initial depth of the CMP. At this depth, the cone tip resistance profiles nearly stabilized for both models despite more oscillations for the SANISAND-F model. The stabilized values are expected to represent the q_c for the given surcharge and material density. The comparison of simulated cone tip resistance profiles suggests that for the current surcharge of 140 kPa and void ratio of 0.88 in Toyoura sand, the DM04 model

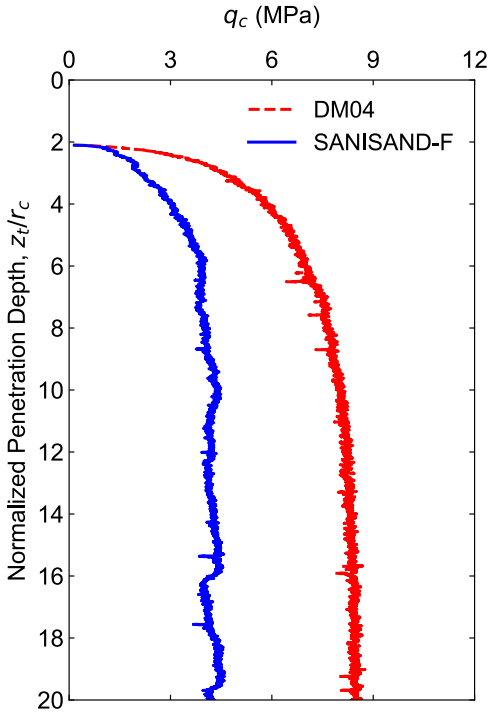

Figure 4. Comparison of cone tip resistance profiles obtained from simulations using DM04 and SANISAND-F models.

reports a q_c of around 8.5 MPa, while the SANISAND-F model reports a value of around 4.5 MPa.

Recall from Fig. 2 that for a void ratio of 0.88, regardless of the level of mean effective stress or Lode angle (triaxial compression or extension, and therefore other values in between the two), the SANISAND-F behaves more contractive than the DM04. This implies that the SANISAND-F generates greater shear-induced volumetric contraction and, consequently, offers less resistance to cone penetration. Therefore, it logically follows that the SANISAND-F exhibits lower cone tip resistance compared to DM04.

To explore the response of the models during cone penetration, the state variable evolutions for the CMP were analyzed in detail, as shown in Fig. 5 for both simulations. In Fig. 5(a), the evolution of the stress ratio $\eta = q/p$ is depicted with respect to the normalized penetration depth z_t/r_c during the cone penetration process, starting from $z_t/r_c = 2$ and concluding at $z_t/r_c = 20$. The critical stress ratio in triaxial compression (M_c) is also shown in this figure for reference. As the cone approaches the CMP, the stress ratio for both models approaches the M_c level. Notably, the SANISAND-F model, characterized by greater shear-induced volumetric contraction as noted earlier, reaches this level later than the DM04.

In Fig. 5(b), the CMP state begins at a dense of critical state for both simulations, indicating a tendency for contraction or dilation in response to changes in the shear stress ratio. This response depends on whether the stress ratio is lower or higher than the phase transformation

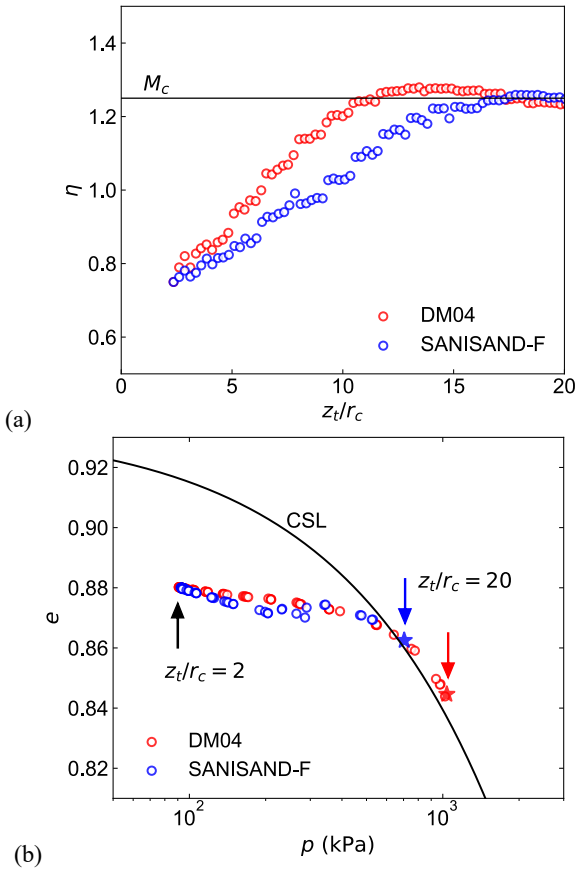

Figure 5. Comparison of variation of material state ($\eta = q/p$, p, and e) at CMP obtained from simulations using DM04 and SANISAND-F models.

slope in the stress space, respectively. During the cone penetration process, both mean and shear stresses increase. Consequently, one would anticipate that the volumetric response is influenced by a balance between the contractive response due to the increase in mean stress and the contractive or dilative response due to variations in the shear stress ratio. It is important to note that the latter is not only observed in the q/p ratio but also in the variations of the stress Lode angle. Specifically, the e–p plot depicts the beginning ($z_t/r_c = 2$) and end ($z_t/r_c = 20$) of the simulation. Notably, at the end of the simulation, the mean stress p reaches a higher level for DM04 than SANISAND-F.

The evolution of the fabric anisotropy, variations of the Lode angle, and proximity of the state to the critical are being studied, and the findings will be discussed in a more extended version of the work.

5. Conclusions

This study employed the DM04 and SANISAND-F constitutive models within the MPM framework of the ANURA3D program to simulate the CPT. The preliminary results demonstrate higher cone tip resistance observed using DM04 compared to SANISAND-F, for the dry deposit of Toyoura sand under an initial vertical stress of 140 kPa and an initial void ratio of 0.88. This difference is attributed to the more contractive response of SANISAND-F at the element level and its impact on the state evolution, leading to a lower level of mobilized stresses.

These outcomes result from considering the evolving fabric anisotropy within the framework of ACST. By illustrating the effect of fabric anisotropy on CPT interpretation, the study advocates for a more informed approach to soil behavior analysis. Further exploration of these initial findings is expected to significantly contribute to the ongoing discourse on geotechnical site characterization, aligning with the industry's movement towards integrating advanced numerical tools to enhance the precision of in-situ assessments and facilitating the safe and efficient design of geotechnical structures.

Acknowledgements

The authors thank Mr. Sheng Zeng and Dr. Jan Machaček for their contributions to the numerical integration of the constitutive models, and Prof. Alba Yerro and her research team for their assistance with navigating the ANURA3D program. Support for this study was provided by the Natural Sciences and Engineering Research Council of Canada (NSERC), SRK Consulting Inc., and Industrias Peñoles.

References

Al-Kafaji, I.K. 2013. "Formulation of a dynamic material point method (MPM) for geomechanical problems", Ph.D. thesis. Dept. of Civil and Environmental Engineering, University of Stuttgart.

Anura3D, 2022. "Anura3D MPM research community", http://www.anura3d.com, Accessed November 15, 2023.

Bardenhagen, S., 2001. "An improved contact algorithm for the material point method and application to stress propagation

in granular material", Computer Modeling in Engineering and Sciences, 2, 509.

Bokkisa, S.V., Macedo, J., Petalas, A.L., Arson, C., 2022. "Assessing static liquefaction triggering considering fabric anisotropy effects under the ACST framework", Computers and Geotechnics, 148, 104796.

Dafalias, Y.F., Manzari, M.T., 2004. "Simple plasticity sand model accounting for fabric change effects", Journal of Engineering Mechanics, 130, 622-634.

Fan, S., Bienen, B., Randolph, M., 2018. "Stability and efficiency studies in the numerical simulation of cone penetration in sand", Geotechnique Letters, 8, 13-18.

Ghasemi, P., Calvello, M., Martinelli, M., Galavi, V., Cuomo, S., 2018. "MPM simulation of CPT and model calibration by inverse analysis", in: Proceedings of the 4th international symposium on cone penetration testing. Amsterdam, The Netherlands. CRC Press, pp. 295-301.

Kouretzis, G.P., Sheng, D., Wang, D., 2014. "Numerical simulation of cone penetration testing using a new critical state constitutive model for sand", Computers and Geotechnics, 56, 50-60.

Li, X.S., Dafalias, Y.F., 2012. "Anisotropic critical state theory: role of fabric", Journal of Engineering Mechanics, 138, 263-275.

Martinelli, M., Galavi, V., 2021. "Investigation of the material point method in the simulation of cone penetration tests in dry sand", Computers and Geotechnics, 130, 103923.

Martinelli, M., Pisano, F., 2022. "Relating cone penetration resistance to sand state using the material point method", Geotechnique Letters, 12, 131-138.

Monforte, L., Arroyo, M., Gens, A., 2022. "Undrained strength from CPTu in brittle soils: A numerical perspective", in: Cone Penetration Testing 2022, CRC Press, pp. 591-597.

Moshfeghi, S., Taiebat, M., Lizcano, A., 2023. "The role of soil constitutive model in simulation of cone penetration test", in: Zdravkovic, L., Kontoe, S., Taborda, D., Tsiampousi, A. (Eds.), Proceedings of the 10th European Conference on Numerical Methods in Geotechnical Engineering (NUMGE 2023), London, UK, doi: 10.53243/NUMGE2023-252.

Moshfeghi, S., Taiebat, M., Lizcano, A., 2024. "Validating the use of material point method and SANISAND model for relating the state parameter with cone tip resistance", in: Stark, N., Evans, T.M. (Eds.), Proceedings of Geo-Congress 2024, Vancouver, BC, Canada, doi: 10.1061/9780784485347.018.

Petalas, A.L., Dafalias, Y.F., Papadimitriou, A.G., 2020. "SANISAND-F: Sand constitutive model with evolving fabric anisotropy", International Journal of Solids and Structures, 188, 12-31.

Pezeshki, A., Ahmadi, M., 2022. "In situ state of tailing silts using a numerical model of piezocone penetration test developed by NORSAND model", International Journal of Geomechanics, 22, 04021264.

Salgado, R., Bisht, V., Prezzi, M., 2022. "Material point method simulations of cone penetration and CPT interpretation", in: Cone Penetration Testing 2022. CRC Press, pp. 16-27.

Taiebat, M., Dafalias, Y.F., 2008. "SANISAND: Simple anisotropic sand plasticity model" International Journal for Numerical and Analytical Methods in Geomechanics, 32, 915-948.

Yoshimine, M., Ishihara, K., Vargas, W., 1998. "Effects of principal stress direction and intermediate principal stress on drained shear behavior of sand", Soils and Foundations, 38, 177-186.

Yost, K.M., Yerro, A., Green, R.A., Martin, E., Cooper, J., 2022. "MPM modeling of cone penetrometer testing for multiple thin-layer effects in complex soil stratigraphy", Journal of Geotechnical and Geoenvironmental Engineering, 148, 04021189.